Modern Applied Science; Vol. 15, No. 1; 2021
ISSN 1913-1844 E-ISSN 1913-1852
Published by Canadian Center of Science and Education

Fourier Transform Infrared and Solid State ^{13}C Nuclear Magnetic Resonance Spectroscopic Characterization of Defatted Cottonseed Meal-Based Biochars

Zhongqi He[1], Mingxin Guo[2], Chanel Fortier[1], Xiaoyan Cao[3] & Klaus Schmidt-Rohr[3]

[1] Southern Regional Research Center, USDA Agricultural Research Service, 1100 Robert E. Lee Blvd., New Orleans, LA 70124, USA

[2] Department of Agriculture & Natural Resources, Delaware State University, Dover, DE 19901, USA

[3] Department of Chemistry, Brandeis University, 415 South Street, Waltham, MA 02453, USA

Correspondence: Zhongqi He, Southern Regional Research Center, USDA Agricultural Research Service, 1100 Robert E. Lee Blvd., New Orleans, LA 70124, USA.

Received: December 15, 2020 Accepted: January 12, 2021 Online Published: January 15, 2021

doi:10.5539/mas.v15n1p108 URL: https://doi.org/10.5539/mas.v15n1p108

Abstract

Conversion to biochar may be a value-added approach to recycle defatted cottonseed meal, a major byproduct from the cotton industry. In this work, complete slow pyrolysis at seven peak temperatures ranging from 300 to 600°C in batch reactors was implemented to process cottonseed meal into biochar products. Elemental analysis, attenuated total reflection Fourier transform infrared (ATR FT-IR) spectroscopy and quantitative solid state ^{13}C nuclear magnetic resonance (NMR) spectroscopy were applied to characterize raw meal and its derived biochar products. The biochar yield and organic C and total N recoveries decreased as the peak pyrolysis temperatures was elevated. However, most of the mineral elements including P in cottonseed meal were retained during pyrolysis and became enriched in biochar as a result of the decreased mass yield. The spectral data showed that pyrolysis removed the functional groups of biopolymers in cottonseed meal, producing highly aromatic structures in biochars. With increasing pyrolysis temperature, alkyl structures decreased progressively in the biochar products and became negligible at higher temperatures (550 and 600°C). Quantitative analysis of FT IR data revealed that the values of a simple 3-band (1800,1700, and 650 cm^{-1})-based R reading of the biochars were linearly related to the pyrolysis temperature, and showed strong correlations with decreasing aromaticity and increasing alkyl, aliphatic C-O/N and carbonyl signal intensities in the ^{13}C NMR spectra. Therefore, the cheaper and faster FT-IR measurement could be used as a routine conversion indicator of pyrolysis of lignocellulosic biomass instead of the more expensive and time-consuming NMR spectroscopy.

Keywords: biochar, cottonseed meal, FT-IR, slow pyrolysis, solid state NMR

1. Introduction

The thermochemical conversion of lignocellulosic biomass using pyrolysis (slow, intermediate, and fast) and gasification results in typically three products: biochar, bio-oil, and syngas (He *et al*., 2016a). The yield of biochar and its ratio to the other two co-products (syngas and bio-oil) are dependent on both the nature of the biomass materials and the carbonization conditions. Slow and intermediate pyrolysis processes with residence times in the minute range are generally favored for biochar production, since the yield of char is linearly correlated with the heating rate of pyrolysis (Mok *et al*., 1992). Persistent in the environment and able to retain water, nutrients, and contaminants, biochar can be used as a soil conditioner for improving soil health, enhancing fertilizer use efficiency, promoting plant growth, and reducing greenhouse gas emission (Guo *et al*., 2016a; 2019). Biochar may also be used in environmental rehabilitation such as remediation of saline soils and reclamation of abandoned mine land through its high capacity for contaminant immobilization (Feng *et al*., 2020; Guo *et al*., 2016a). Biochar filters are suitable for onsite wastewater treatment (Perez-Mercado *et al.*, 2018; Dalahmeh *et al.*, 2020). In "green" chemistry, biochar is used as an enzyme carrier or immobilizer to increase the enzymatic activity and thermal stability (Noritomi *et al*., 2019; Noritomi *et al*., 2018; Noritomi *et al.*, 2017).

Cotton is a non-food crop and a major fiber source for the textile industry. Exploration of the utilization of cotton plant biomass residues as a sustainable industrial feedstock promises to enhance the environmental and economic viability of the cotton industry (Grewal *et al*., 2020; He *et al*., 2020; 2017; Windeatt *et al*., 2014). Especially, defatted cottonseed meal, the solid byproduct after oil extraction from cottonseed, accounts typically for 45% of the cottonseed biomass and is currently mainly used as an animal feed additive (Swiatkiewicz *et al*., 2016; Cheng *et al.,* 2020) and fermentation substrate (Grewal & Khare, 2017). Attempts have been made to convert cottonseed meal into value-added products such as bioplastics and films (Chen *et al*., 2019), superabsorbent hydrogel (Zhang *et al*., 2010), antioxidant peptides/extracts (Song *et al*., 2020), and wood adhesives (Cheng *et al*., 2013; He *et al*., 2014a, b; Li *et al*., 2019; Liu *et al*., 2018). The economic viability of these biorefinery efforts, however, is still a major concern. Given its relatively high energy density (i.e., higher heating value of 17.9 MJ kg^{-1}), cottonseed meal could be a good feedstock for producing biochar and bio-oil via pyrolysis (He *et al*., 2016a; Ozbay *et al*., 2001). While there were several reports from Turkey (Ozbay *et al*., 2006; Putun, 2010; Putun *et al*., 2006) and India (Singh *et al*., 2014) on pyrolysis of cottonseed cakes (equivalent to the meal product in the USA) mainly for bio-oil production, pyrolysis processing of cottonseed meal had not been investigated in the USA.

Therefore, we conducted cottonseed meal pyrolytic conversion studies, aiming to facilitate the utilization of this agricultural byproduct as a "green" and value-added raw material. Previously we (He *et al*., 2018) characterized the cottonseed meal-derived bio-oil products for potential use as adhesives blends like other pyrolysis bio-oils (Li *et al.*, 2020a; Mao *et al*., 2017; Wan *et al*., 2018). In this work, using attenuated total reflection Fourier transform infrared (ATR FT-IR) spectroscopy and quantitative solid state ^{13}C nuclear magnetic resonance (NMR) spectroscopy, we characterized meal-derived biochar products prepared at seven peak temperatures in the range of 300 to 600°C. The goals of this project were to 1) increase the knowledge on the effects of pyrolysis temperature on the chemical composition of the meal-based biochar products and 2) explore a structural indicator measurable by relatively simple FT-IR spectroscopy.

2. Experimental

2.1 Cottonseed Meal Material and Slow Pyrolysis

Mill-scale produced cottonseed meal was provided by Cotton, Inc. (Cary, NC, USA) and was used as the biomass material for pyrolysis (He *et al*., 2016b). The cottonseed meal was converted to biochar and bio-oil using a custom-made benchtop pyrolyzer consisting of a furnace, a pyrolysis reactor (a 3.78-L iron container with a side vent and movable lid), a condenser, and a bio-oil collector (Guo *et al*., 2012). Approximately 2200 g of the air-dried cottonseed meal were packed into the reactor. The reactor was then placed in the electricity-powered furnace. Pyrolysis of cottonseed meal started when the temperature inside the reactor reached above 200°C. The resulting pyrolysis vapor passed through the side vent and entered into the condenser, where a room temperature of 22°C was maintained by slowly flowing water. Slow pyrolysis with peak temperature at 300, 350, 400, 450, 500, 550, and 600°C was applied to conversion of cottonseed meal to biochar and bio-oil. Hereafter, the resulting biochars are referred to as Char300, Char350, Char400, Char450, Char500, Char550, and Char600, respectively. At each peak temperature when the pyrolysis was complete as indicated by no more visible smoke accumulating in the condenser, the reactor was withdrawn from the furnace and immediately sealed with a piece of aluminum tape on the side vent. After cooling down to room temperature, the biochar in the reactor was ground to <0.85 mm and stored in a Ziploc bag for later chemical and spectroscopic characterization.

2.2 Determination of Elemental Contents

The contents of total N and C in each sample were determined using a LECO Truspec dry combustion Carbon/Nitrogen Analyzer (St. Joseph, MI) (NFTS, 1993). The total contents of 11 other mineral elements (P, Ca, K, Mg, Na, S, Fe, Zn, Cu, Mn, and Al) were analyzed by digesting the biochar samples with HNO_3 in the HotBlock Environmental Express block digester followed by quantitative measurements using a Spectro CirOs inductively coupled plasma (ICP) spectrometer (Mahwah, NJ, USA) (He *et al*., 2017). Triplicates were analyzed for each sample and data of means were reported.

2.3 ATR FT-IR Spectroscopy

Raw cottonseed meal and the derived biochars were analyzed by an ATR FT-IR spectrometer equipped with the OPUS software (Bruker Optics, Billerica, MA, USA). An amount of 5-10 mg of sample was placed on the diamond/ZnSe ATR crystal, enough to cover the crystal entirely, which was subsequently secured with a metal clamp to ensure a reproducible pressure applied to the samples and intimate contact between the ATR crystal and the sample. All samples were analyzed in the reflectance mode. Samples were run against an air background with 32 sample scans at 8 cm^{-1} resolution in the mid-infrared region (600 cm^{-1}-4400 cm^{-1}). Spectra were

generated using the Origin software (Version 8). All spectra were baseline corrected and integrated using peak height. Peak heights were calculated from the baseline using the Bruker OPUS FT-IR software. Using a simple 3-band algorithm, R readings were calculated based on the intensity ratio of a multi-point average (A_{1700}) of bands in the 1750-1500 cm^{-1} region relative to the average (A_{650}) of bands in the 645-655 cm^{-1} region, both after subtracting the average (A_{1800}) of reference bands in the 2000-1790 cm^{-1} region (Liu *et al*., 2015).

2.4 Solid State ^{13}C NMR Spectroscopy

Solid state ^{13}C NMR analyses of cottonseed meal and the derived biochars were performed at 100 MHz using a Bruker Avance 400 spectrometer equipped with a 4-mm double-resonance probe head (Cao *et al*., 2019). Nearly quantitative multiple cross-polarization (multiCP) ^{13}C NMR spectra (Johnson & Schmidt-Rohr, 2014) were measured on cottonseed meal and seven cottonseed meal-derived biochar samples with 11 cross-polarization repeats of 0.55 ms to 1.1 ms duration each. Quantitative direct polarization (DP) ^{13}C NMR spectra were recorded for cottonseed meal chars prepared at 550 °C and 600 °C with recycle delays of 25 s and 20 s, respectively. MultiCP and DP were also combined with recoupled dipolar dephasing (Mao & Schmidt-Rohr, 2004) to obtain quantitative information on the nonprotonated carbons, and mobile segments such as rotating CH_3 groups and $(CH_2)_n$ in lipids.

Peak assignments were based on the literature for agricultural byproducts and soil organic matter (Cao *et al*., 2011; He & Mao, 2011; He *et al*., 2015a). Specifically, the assignments for cottonseed meal spectra were 220-187 ppm → C=O, 187-163 ppm → carboxyls and amides, 163-141 ppm → aromatic C-O, 141-113 ppm → aromatic C-C and C-H, 113-94 ppm → O-C-O, 94-46 ppm → alkyl C-O/N, 46-0 ppm → alkyl C, and 27-0 ppm → CH_3. Peak assignments for biochar products were shifted slightly as 220-187 ppm → C=O, 187-165 ppm → carboxyls and amides, 165-90 ppm → aromatics including nonprotonated aromatic C-O/N and protonated aromatic C-H, 90-50 ppm → alkyl C-O/N, 50-0 ppm → alkyl C, and 27-0 ppm → CH_3.

3. Results and Discussion

3.1 Yield and Element Contents of Biochar Products

Table 1. Production yield (%), contents (g kg^{-1}) and recovery (%) of organic C, total N, and total P of biochar products and raw material defatted cottonseed meal (CSM). Pyrolysis temperatures of CSM are indicated by the suffixing numbers of char products.

Product	Yield	Organic C		Total N		Total P	
		Content	Recovery	Content	Recovery	Content	Recovery
CSM	N/A	465.4±4.2	N/A	72.3±4.2	N/A	12.7±4.2	N/A
Char300	53.3	556.0±4.2	63.7	89.8±4.2	66.2	22.7±4.2	99.6
Char350	46.7	367.6±4.2	36.9	71.7±4.2	46.3	24.0±4.2	99.8
Char400	40.8	302.4±4.2	26.5	58.7±4.2	33.1	26.3±4.2	100.4
Char450	36.0	255.2±4.2	19.8	53.3±4.2	26.5	26.6±4.2	96.2
Char500	35.0	255.7±4.2	19.2	50.1±4.2	24.2	27.9±4.2	96.1
Char550	33.4	258.3±4.2	18.5	46.7±4.2	21.6	29.8±4.2	97.9
Char600	32.2	253.5±4.2	17.5	42.1±4.2	18.7	30.5±4.2	87.5

Biochar yield, contents of organic carbon (OC), total N, and total P in and its biochar products are listed in Table 1. The yield of biochar decreased from 53.33% of the dry feed mass to 32.16% with increases in pyrolysis temperature from 300 to 600°C. Recoveries of OC and total N were in the same decreasing trend. However, the biochar prepared at 300°C possessed OC and total N contents even higher than those of raw cottonseed meal indicating enriched organic carbon and N-compounds in Char300. Higher pyrolysis temperature converted biomass to more volatile hydrocarbons (with or without N) and non-condensable gases, leading to decreases in mass yield and OC and N recoveries (He *et al*., 2016a). Phosphorus is mainly present in cottonseed meal as phosphate ester compounds (He *et al*., 2015; 2017). The pyrolytic products were predominantly non-volatile inorganic phosphates, leading to nearly 100% P recovery and increasing total P contents in biochars as the pyrolysis temperature was elevated. The relatively low P recovery (87.5%) with Char600 might be due to some mass deviation as the low recovery was not observed with the content of P in poultry litter-based Char600 (Guo *et al*., 2012). Nowadays, P is not only a critical plat nutrient, but also a pollutant of concern with excess quantity in the environment (He *et al*., 2016c; Adhikari *et al*., 2019). Sequential extraction of P in biosolids and resultant

biochars showed that P becomes more tightly bound to biochar after pyrolysis, particularly at increased process temperature (Jiang *et al*., 2019). Investigating P speciation transformation during pyrolysis of poultry litter, they reported that organic P (in particular phytates) in poultry litter was decomposed to inorganic P forms at a pyrolysis temperature above 300°C while hydroxyapatite ($Ca_{10}(PO_4)_6(OH)_2$) was formed in the biochar products. Furthermore, the inhibition effect of pyrolysis on P lability occurs mainly through transformation of labile phosphates in poultry litter into less soluble forms. While both poultry litter and cottonseed meal are phytate-enriched, future characterization by wet chemistry (He & Honeycutt, 2001) and spectroscopic techniques (He *et al*., 2009a) should shed light on the P species and bioavailability in these cottonseed meal-derived biochars.

In addition, we also measured the contents of 10 other mineral elements in cottonseed meal and its derived biochar products (Table 2). The data for cottonseed meal were in the range of defatted cottonseed meal products in the literature *(*He *et al.,* 2016b, 2015b). Compared to the meal, the contents of the macro mineral nutrients Ca, K, Mg and the micro mineral nutrients Fe, Zn, Mn in the seven biochars increased by 2- to 3-fold, to a greater extent at higher pyrolysis temperature. This trend was apparently due to the non-volatile properties of these mineral compounds in the 300-600°C temperature range, and increased concentration from reduced biochar mass at higher pyrolysis temperature. The contents of Na and Cu also increased in the biochar products. However, the increasing trend with higher pyrolysis temperature was not obvious, perhaps partly due to the greater measurement deviations with their lower content and less measurement sensitivity. On the other hand, there was a lower Al content in all biochar products than cottonseed meal itself, and the content values fluctuated. While Al compounds seem non-volatile, they appear to be distributed to the bio-oil fractions as the previous work on the bio-oil characterization reported 73.7 and 391.1 mg Al kg^{-1} of aqueous and oily phases of bio-oil, compared to 99.6 mg Al kg^{-1} of the meal (He *et al*., 2018). In the meantime, the content of the non-metal element S in biochar products also decreased with increasing pyrolysis temperature and all were lower than in the meal. As S existed in the meal primarily in S-containing protein/amino acids (He *et al*., 2015b; 2014c), pyrolysis apparently decomposed these protein/amino acids and released the S in volatile S compounds. This observation was different from that for poultry litter-based biochars, whose S content was 10-30 fold higher and increased with higher pyrolysis temperatures (Guo *et al*., 2012). The difference could be attributed to the fact that significant sodium bisulfate was intentionally added to poultry bedding to reduce feces ammonia emissions (Guo *et al*., 2009). Indeed, the contents of mineral elements were generally higher in animal manure-based biochars (Guo *et al*., 2019; 2012; Zeng *et al*., 2018) due to mineral supplements in animal feeds and manure treatments (Schroder *et al*., 2011; Zhang *et al*., 2020)

Table 2. Contents of 10 selected elements in cottonseed meal (CSM) and its biochar products. Pyrolysis temperatures of CSM are indicated by the suffixing numbers of char products.

Product	Ca	K	Mg	Na	S	Fe	Zn	Cu	Mn	Al
	----------Macro element, g kg^{-1}----------					----------Micro element, mg kg^{-1}----------				
CSM [a]	2.3±0.0	15.5±0.1	6.2±0.0	2.3±0.0	4.2±0.0	107±2	59±1	9.4±0.1	23.3±0.6	99.6±6.8
Char300	3.9±0.1	29.6±0.1	12.4±0.2	2.4±0.0	3.0±0.0	136±6	139±13	31.0±2.4	54.8±0.6	0.0±0.0
Char350	4.5±0.1	33.5±0.3	14.4±0.2	2.8±0.0	2.7±0.1	190±6	154±10	26.3±3.9	63.4±0.6	0.0±0.0
Char400	4.2±0.1	31.6±0.4	13.7±0.1	2.6±0.0	2.2±0.1	215±7	152±10	22.7±3.1	59.0±0.7	14.4±0.8
Char450	5.2±0.1	38.8±0.4	16.5±0.2	3.0±0.0	2.0±0.0	218±4	175±11	17.1±0.8	69.3±0.9	2.5±0.5
Char500	5.1±0.0	38.6±0.2	16.6±0.3	3.1±0.0	1.8±0.0	219±2	171±10	15.1±1.0	69.5±0.7	4.7±0.3
Char550	5.9±0.1	42.4±0.5	18.6±0.3	3.2±0.0	1.4±0.0	---[b]	211±5	18.4±4.1	86.9±1.9	22.3±1.1
Char600	5.7±0.1	41.1±0.3	18.2±0.2	3.2±0.0	1.0±0.0	260±6	200±10	17.5±1.7	75.0±1.2	30.8±1.1

[a] Data taken from He *et al*. (2018).

[b] No reliable data available.

3.2 ATR FT-IR Spectra

Figure 1 presents the ATR FT-IR spectra of cottonseed meal (CSM) and the seven biochar products in the functional region from 2700 to 4000 cm^{-1} and the fingerprint region from 500-2000 cm^{-1}. The FT-IR spectral features of the meal samples were consistent with those reported previously (He *et al*., 2014b). The raw cottonseed meal showed a main absorption peak at 3280 cm^{-1} and double shoulders around 2900 cm^{-1} in the functional region of 2700-4000 cm^{-1}. These spectral features could be assigned to C-H bond stretching and O-H bond stretching,

respectively (He & Zhang, 2015; Waldrip *et al.*, 2014). In the biochar products, the double shoulders around 2900 cm^{-1} dwindled with increasing pyrolysis temperature, indicating the gradual diminishing of aliphatic functional group in these biochar products. Due to the hydrophobic nature of aliphatic groups, the relative intensity of the double or triple shoulders around 2900 cm^{-1} is regarded as an indicator of wettability (He *et al*., 2011; Smidt *et al*., 2002). This wettability feature was consistent with the spectral difference between the lipid-rich whole cottonseed and its defatted cottonseed meal as its double shoulders was much weaker compared to those of whole cottonseed reported previously (Liu *et al*., 2016). Thus, it is reasonable to conclude that the wettability of meal-derived biochar generally decreases as the pyrolysis temperature increases. In the fingerprint region, the major peaks at 1535 and 1236 cm^{-1} in the meal spectrum were attributed to C-N stretching and N-H bending of amide bonds of proteins (He *et al.*, 2014b). These two bands in the spectra of the biochar products became weaker and eventually diminished with increased pyrolysis temperature. The peaks at 1632, 1401 and 1399 cm^{-1} could be assigned to a diversity of C-O and C=C containing functional groups such as carboxylic acids esters, ketones, anhydrides , and aromatic moieties of the amino acids, lipids, and carbohydrates in cottonseed meal (Haeldermans *et al.*, 2019; He *et al*., 2014b; Younis *et al*., 2017). The spectra of biochars showed the same features, but became weaker at higher pyrolysis temperature, indicating greater stability of aromatic linkages than other functional components (Jiang *et al*., 2019; Bekiaris *et al*.; 2020). Compared to the meal, the relative stronger bands of aromatic ring structures in the range from 900 to 650 cm^{-1} in the biochars further confirmed the observation.

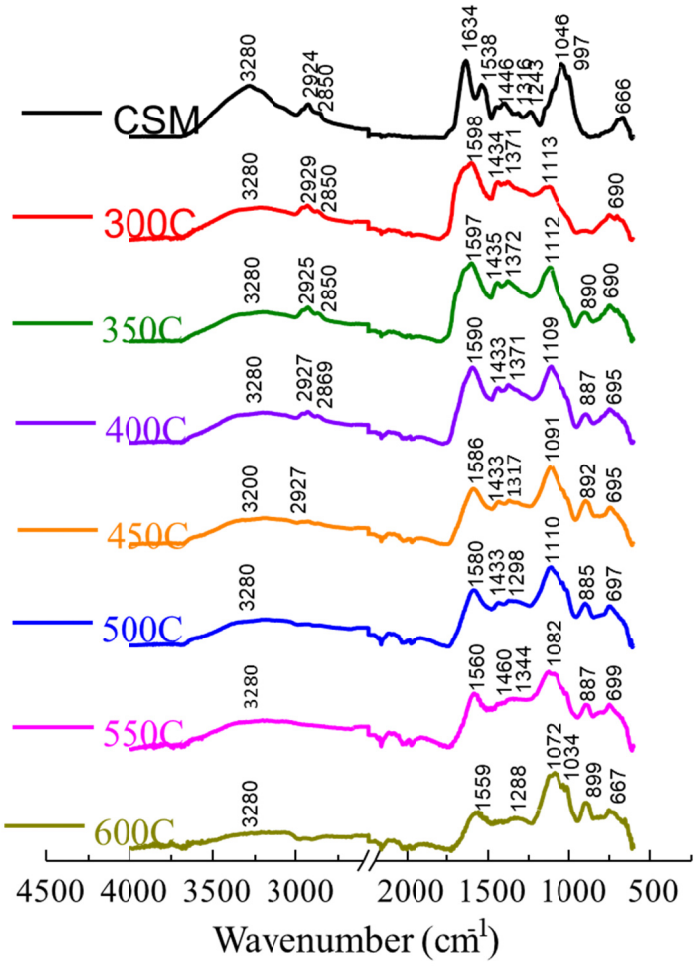

Figure 1. ATR FT-IR spectra of defatted cottonseed meal (CSM) and its biochars produced at the seven indicated pyrolysis temperatures

The peak at 1042 cm^{-1} in the spectrum of cottonseed meal upshifted and gradually split into two bands in the biochars with the FT-IR features of phosphate compounds (He *et al*., 2007). The peak at 1042 cm^{-1} of the meal was contributed from carbohydrates and phosphate compounds (He *et al*., 2006). Pyrolysis decomposed carbohydrates and enriched non-volatile P compounds in biochars (Table 1) which subsequently intensified the peak. However,

FT-IR spectroscopy could not identify the specific P species due to the high similarity of spectral features of different P compounds (He *et al*., 2007). By solid state ^{31}P NMR analysis, Jiang et al. (Jiang *et al*., 2019) found that organic phytates (inositol hexaphosphoric acid compounds) decomposed and hydroxyapatite [$Ca_{10}(PO_4)_6(OH)_2$] formed during conversion of poultry litter to biochar at pyrolysis temperatures above 300 °C, in addition to the formation of farringtonite [$Mg_3(PO_4)_2$]. As the meal is phytate-rich (Han, 1988) and possesses significant base metal minerals with contents of K>Mg>Ca (Table 2), future work with wet chemistry and ^{31}P NMR spectroscopy (He & Honeycutt, 2001; He *et al*., 2009a) could shed light on what metal P species had been formed in biochars from meal phytates.

In application of ATR FT-IR spectroscopy to characterize biochars generated from various agricultural by-products, Liu *et al.* (2015) proposed a simple 3-band algorithm (R readings) per multi-point averages of the band intensities at respective ranges of 1750-1500 cm^{-1}, 2000-1790 cm^{-1}, and 645-655 cm^{-1}. While the FT-IR analysis of Liu *et al*. (2015) has been applied to qualitative characterization of biochars from various agricultural and industrial wastes and byproducts (e.g., Li *et al.*, 2020b; Nair *et al.*, 2020; Rodriguez *et al.*, 2020), the quantitative evaluation by the R reading has not been adopted. This is mainly due to the two facts that 1) its physical significance is not apparent as the idea was derived from three-band ratio algorithms in cotton fiber and cellulose studies (Liu *et al.*, 2011; Nam *et al.*, 2017), and 2) Liu *et al*. (2015) did not report clear correlations between R readings and pyrolysis temperature of the four types of plant biomass biochars they generated.

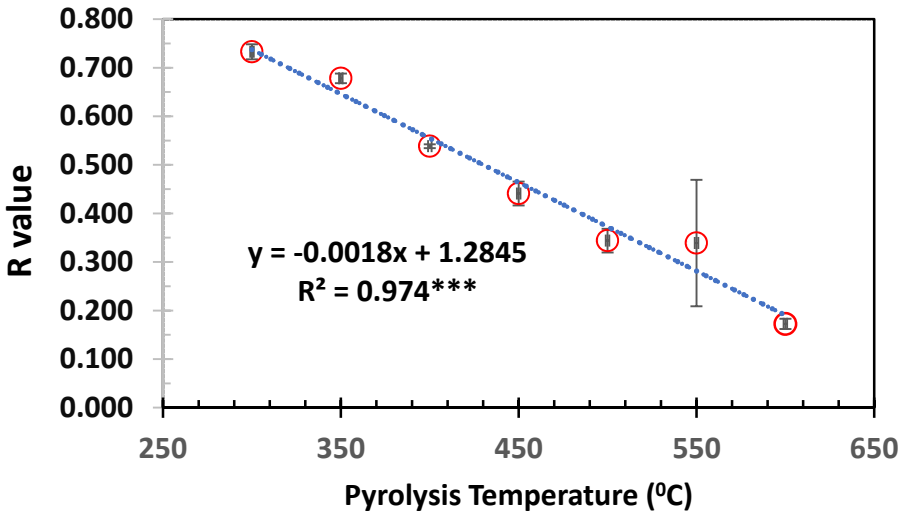

Figure 2. Effect of pyrolysis temperatures on 3-band R readings of cottonseed meal-based biochar products. R=(A_{1700}-A_{1800})/(A_{650}-A_{1800}) (Liu *et al*., 2015). The symbol *** indicates that the statistical R-squared value is significant at p= 0.001

To explore its potential application, in this work, we computed the R readings of the seven meal-based biochars (Figure 2). The R value was 0.516±0.030 for the raw meal. In comparison, the R reading of Char300 was notably higher at 0.735. The value decreased linearly for biochars generated at elevated pyrolysis temperatures. Char600 demonstrated an R reading at 0.175. The reported R reading values of lignocellulosic residues-derived biochars were in the range of 0.65 and 0.20 for lower pyrolysis temperature (300 to 500°C) products and 0.11 to 0.03 for higher temperature (600 to 800°C) products (Liu *et al*., 2015). Furthermore, we noticed a linear regression relationship (R^2 =0.974, p < 0.001) between the R reading of meal-derived biochar and the pyrolysis peak temperature, suggesting pyrolysis temperature is a key factor controlling the spectral R reading of biochar products. The apparent cause was inclusion of the R readings of the raw feedstock materials in the correlation analysis. The well fitting linear regression found in this work indicated that the FT-IR spectral intensity difference could be used to distinguish semi-quantitatively lignocellulosic material-based biochar products prepared under different conditions.

3.3 Solid State ^{13}C NMR Spectra

The multiple cross-polarization (multiCP) ^{13}C NMR spectra of cottonseed meal and the derived biochar products are presented in Figure 3. The resulting nearly quantitative data are listed in Table 3. The NMR spectra of raw

cottonseed meal are typical of organic compound samples (He *et al*., 2009b; Ranatunga *et al*., 2017). Its peaks could be

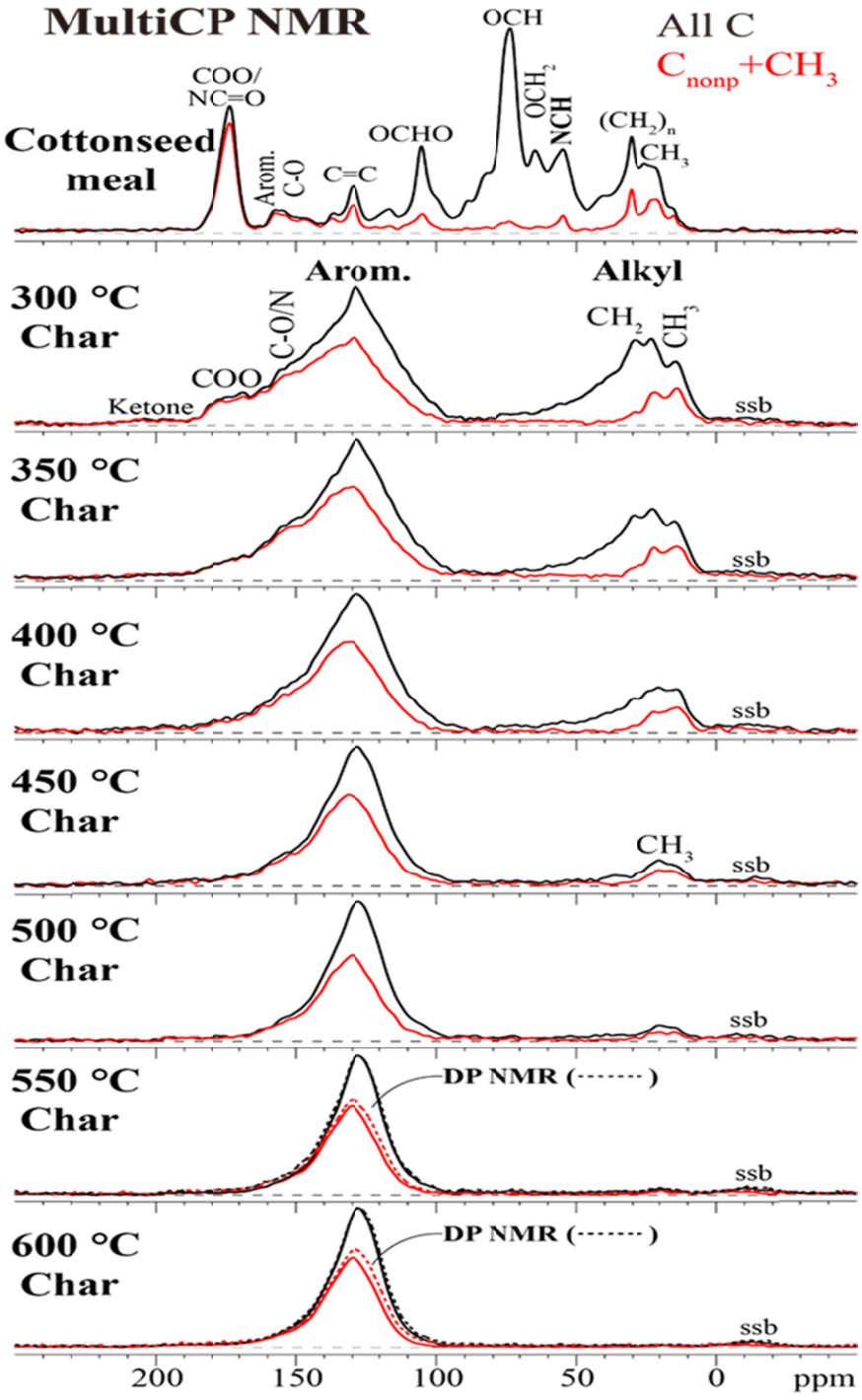

Figure 3. Solid state multiple cross-polarization (multiCP) ^{13}C NMR spectra of defatted cottonseed meal and its biochars produced at the seven indicated pyrolysis temperatures

assigned to seven major functional groups: (1) alkyl carbons, with the signals near 20 ppm assigned to methyl in hemicellulose and gossypol, the shoulder at ~15 ppm assigned to methyl end groups in lipids, and the sharp peak near 30 ppm to $(CH_2)_n$ in lipid; (2) methoxyl (OCH_3) and NCH carbons resonating at ~55 ppm; (3) O-alkyl carbons including OCH_2 groups (C6 carbons of cellulose) near 64 ppm, OCH groups (C2, C3 and C5 carbons of cellulose or hemicellulose) near 72 ppm, and OCH groups (C4 carbons of cellulose) displaying shoulders at 82 ppm and 88 ppm; (4) di-O-alkyl carbons with a sharp peak near 105 ppm; (5) C=C carbons and nonoxygenated aromatic carbons around 110-140 ppm; (6) oxygenated aromatic carbons resonating at 148 ppm and 156 ppm; and (7)

carboxyl/amide groups resonating near 173 ppm. In addition, the signals of OCH_3 are partially selected and retained in the dipolar-dephased spectrum, with its low intensity indicating a smaller contribution of OCH_3 than NCH to the peak near 55 ppm. Per the chemical composition of the meal (He *et al*., 2015b), the identified signals were more specifically indicative of the presence of cellulose or hemicellulose (20, 64, 74, 82, 88, and 105 ppm), peptide/protein (55 and 173 ppm), and lipid (15, 30, and 129 ppm) in the cottonseed meal.

The ^{13}C NMR spectra of biochars produced from cottonseed meal are composed of two major broad bands, assigned to aromatic and alkyl carbons, respectively. These features were similar to those of lignocellulosic material-based (Cao *et al*., 2019; Haeldermans *et al*., 2019) and manure-based (Cao *et al*., 2011; Jiang *et al*., 2019) biochar products. For the biochars prepared at low temperature (< 400°C), the aromatic carbon peak extended to ~190 ppm due to the overlapping of signals from nonpolar aromatics, O/N-substituted aromatics and carboxyl/ester (COO). The alkyl carbon band showed signals primarily from CH_3, and CH_2/CH. These observations indicated that pyrolysis even at the lowest temperature (300°C) had transformed biopolymers present in cottonseed meal to aromatic-rich structures. With increasing temperatures, the aromatic band became much narrower, resulting from the decreased intensity of O/N-substituted aromatics and carboxyl/ester (COO) (Table 3). The alkyl C band, dominated by signals of CH_3 above 400°C, decreased in intensity with temperature and became negligible at 550 and 600°C. Furthermore, comparison of DP (dashed lines) and multiCP spectra of Char550 and Char600 showed that multiCP provided nearly quantitative spectra in much shorter measuring time while the proportion of nonprotonated aromatic carbons was only slightly underestimated. In summary, pyrolysis of the meal at 300 °C removed its signatures of biopolymers, and produced highly aromatic structures. With increasing temperature, alkyl structures (mainly CH_3 for biochars prepared at above 400°C) decreased progressively in intensity and became negligible at high temperatures (550 and 600°C). Meanwhile, O/N-substituted aromatics and carboxyl/ester decreased in intensity, leading to more uniform aromatic ring structures.

Table 3. Nearly quantitative ^{13}C NMR spectral analysis (% of total ^{13}C signal) of defatted cottonseed meal (CSM) and its pyrolysis biochars from multiCP spectra and multiCP spectra after dipolar dephasing. Pyrolysis temperatures of CSM are indicated by the suffixing numbers of char products.

Product	Carbonyls		Aromatics [b]			Aliphatic C-O/N [b]		Alkyl	
	C=O	COO	C-O/N	C-C	C-H	O-C-O	C-O/N	C_q/CH/CH_2	CH_3
CSM	0.0	14.0	3.5	3	4	9	46	14	6.5
Char300	1.0	5.5	39.0		21.0	5.5		17.5	10.5
Char350	1.0	4.0	46.0		20.0	4.0		15.0	10.0
Char400	1.5	3.5	49.0		25.0	3.0		9.0	9.0
Char450	1.0	3.0	56.0		28.0	2.0		3.5	6.5
Char500	0.5	1.5	54.0		34.0	2.5		3.0	4.5
Char550	0.5	1.0	60.0		32.5	2.5		1.5	2.0
Char550[a]	0.5	2.0	63.0		28.5	2.5		1.5	2.0
Char600	1.0	2.0	62.5		32.0	1.0		0.5	1.0
Char600[a]	1.0	2.0	66.0		27.0	2.0		1.0	1.0

[a] Functional group composition derived from quantitative ^{13}C direct polarization magic angle spinning spectra.

[b] Different sub types of two functional groups (i.e., aromatics between C-O/N and C-C, and aliphatic C-O/N between O-C-O and C-O/N) indistinguishable with biochar products.

3.4 Correlation Analysis of Quantitative FT-IR and Solid State ^{13}C NMR Spectral Data

While both FT-IR and solid state ^{13}C NMR spectroscopies are complementarily used in the characterization of agricultural and soil samples, the two types of data are generally compared only qualitatively in terms of their functional group assignments (He *et al*., 2009b; Jiang *et al*., 2019; Mao *et al*., 2008). Instead, in this work, we quantitatively analyzed the correlation of the data of FT-IR 3-band R readings and ^{13}C NMR functional group concentrations of seven meal-based biochar products (Figure 4).

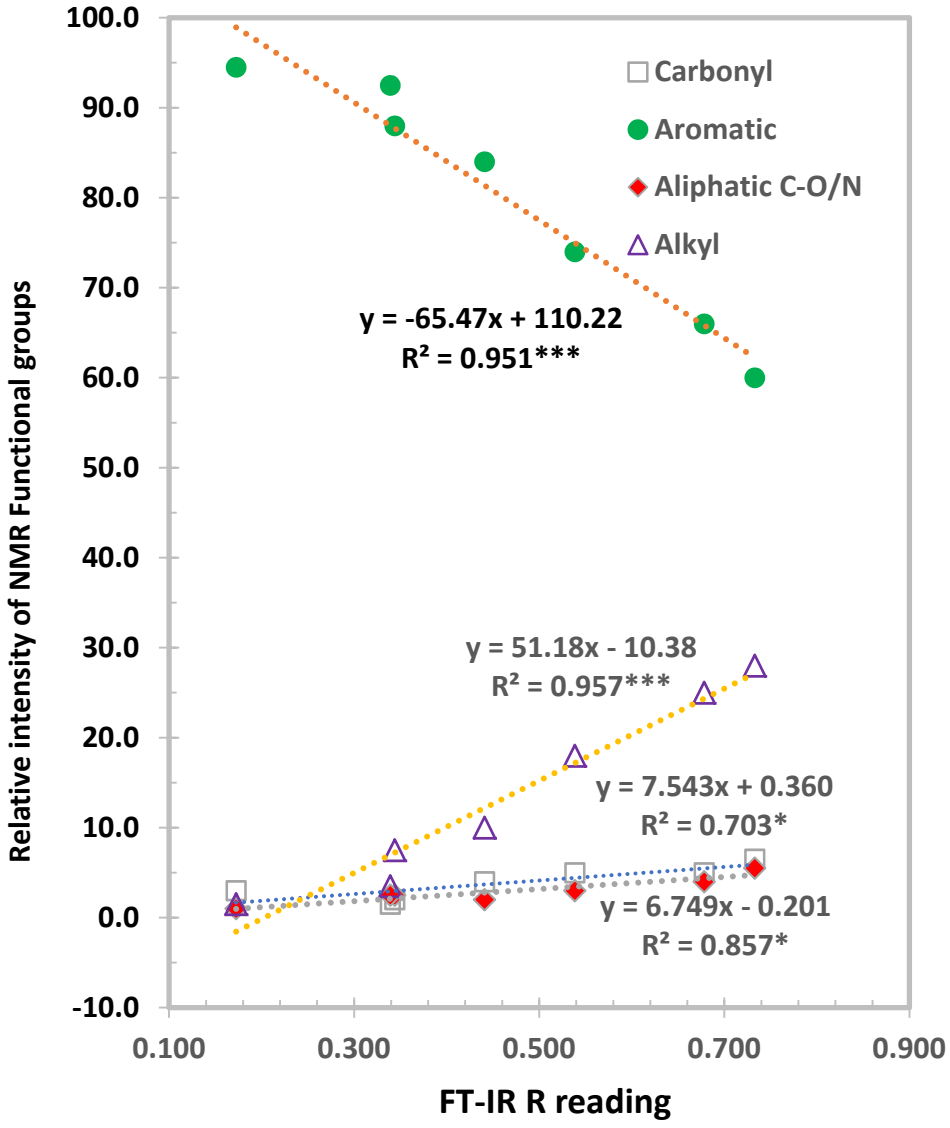

Figure 4. Linear regressions of FT-IR 3-band R readings with relative intensities of ^{13}C NMR functional groups of cottonseed meal-based biochar products. Symbols * and *** indicate the statistical R-squared values significant at p=0.05 and 0.001, respectively

FT-IR 3-band R readings showed a negatively linear regression with the aromatic carbon fraction from ^{13}C NMR spectroscopy with high confidence (R^2 = 0.951, p=0.001). The FT-IR R readings showed a linear relationship with other three carbon functional group concentrations from ^{13}C NMR spectroscopy. The R-squared values for the regressions with alkyl, aliphatic C-O/N and carbonyl were 0.951, 0.857, 0.703 with p=0.001, 0.05 and 0.5, respectively. These observations suggested that the aromatic components in these biochars were mainly from alkyl components with some contributions from aliphatic C-O/N and carbonyl components in cottonseed meal. Given that more chemically detailed and quantitative information can be deduced from solid state ^{13}C NMR spectra, Haeldermans and coworkers (Haeldermans *et al*., 2019) argued that the technique is more convenient than FT-IR to monitor the pyrolysis conversion of the lignocellulosic material into the biochar. Hereby in our work, the high correlation between the two sets of data implied that the more affordable and faster FT-IR R measurement developed by (Liu *et al.,* 2015) could be used as a routine conversion indicator of pyrolysis of lignocellulosic biomass if further confirmed with biochars from other feedstocks.

4. Conclusions

To our knowledge, this work is the first reporting on characterization of cottonseed meal-based biochar products, though a few publications on meal-derived pyrolysis bio-oil products can be found in the literature. Both content and recovery of OC and total N in meal-derived biochars decreased with increasing pyrolysis temperature. However, P and most other mineral elements in the feedstock were retained and concentrated in the biochars. ATR FT-IR and solid state ^{13}C NMR analyses indicated that cottonseed meal was primarily composed of cellulose, hemicellulose, protein, and lipid. Slow pyrolysis of cottonseed meal at 300°C removed signatures of the oxygen-containing biopolymers and subsequently produced highly aromatic structures. With increasing pyrolysis temperatures, the nonpolar alkyl structures decreased progressively and became negligible at 550 and 600°C, leading to more uniform aromatic ring structures in high-temperature biochar products. This information is useful for guiding the effective uses of these products as soil amendments, industrial feedstocks, and for environmental remediation. For example, the higher pyrolysis temperatures would be selected for production of the cottonseed meal biochar products for carbon sequestration and other environmental applications as the adsorption capacity is due to the abundance of polar functional groups on the carbon material surface (Song & Guo, 2012; Kalus *et al.*, 2019). On the other hand, lower temperatures (e.g., 300°C) should be considered in pyrolysis for agricultural use to retain plant nutrients, N uptake and organic matter diversity (Guo *et al.*, 2016b; Mahdi *et al.*, 2017).

In addition, a simple 3-FT-IR-band (1800, 1700, and 650 cm^{-1})-based algorithm provided R readings of the biochars that were shown to be linearly related to the pyrolysis temperature, indicating pyrolysis temperature as a key factor affecting the readings. Furthermore, the readings showed a negative linear regression with the relative intensity of ^{13}C NMR-identified aromatic structures, and positive linear regressions with ^{13}C NMR-identified functional groups of alkyl, aliphatic C-O/N and carbonyl. If further confirmed, the more affordable and faster FT-IR R measurement could be used as a routine conversion indicator of pyrolysis of lignocellulosic biomass instead of the expensive and time-consuming solid state ^{13}C NMR spectroscopy.

References

Adhikari, S., Gascó, G., Méndez, A., Surapaneni, A., Jegatheesan, V., Shah, K., & Paz-Ferreiro, J. (2019). Influence of pyrolysis parameters on phosphorus fractions of biosolids derived biochar. *Sci. Total Environ., 695*, 133846. https://doi.org/10.1016/j.scitotenv.2019.133846

Bekiaris, G., Peltre, C., Barsberg, S. T., Bruun, S., Sørensen, K. M., Engelsen, S. B., Magid, J., Hansen, M., & Jensen, L. S. (2020). Comparison of three different FTIR sampling techniques (diffuse reflectance, photoacoustic and attenuated total reflectance) for the characterisation of bio-organic samples. *J. Environ. Qual., 49*, 1310-1321. https://doi.org/10.1002/jeq2.20106

Cao, X., Ro, K. S., Chappell, M., Li, Y., & Mao, J. (2011). Chemical structures of swine-manure chars produced under different carbonization conditions investigated by advanced solid-state 13C nuclear magnetic resonance (NMR) spectroscopy. *Energy Fuels, 25*(1), 388-397. https://doi.org/10.1021/ef101342v

Cao, X., Xiao, F., Duan, P., Pignatello, J. J., Mao, J., & Schmidt-Rohr, K. (2019). Effects of post-pyrolysis air oxidation on the chemical composition of biomass chars investigated by solid-state nuclear magnetic resonance spectroscopy. *Carbon, 153*, 173-178. https://doi.org/10.1016/j.carbon.2019.07.004

Chen, W., Ding, J., Yan, X., Yan, W., He, M., & Yin, G. (2019). Plasticization of cottonseed protein/polyvinyl alcohol blend films. *Polymers, 11*(12), 2096. https://doi.org/10.3390/polym11122096

Cheng, H. N., Dowd, M. K., & He, Z. (2013). Investigation of modified cottonseed protein adhesives for wood composites. *Ind. Crop. Prod., 46*, 399-403. https://doi.org/10.1016/j.indcrop.2013.02.021

Cheng, H. N., He, Z., Ford, C., Wyckoff, W., & Wu, Q. (2020). A review of cottonseed protein chemistry and non-food applications. *Sustain. Chem., 1*, 256-274. https://doi.org/10.3390/suschem1030017

Dalahmeh, S. S., Stenström, Y., Jebrane, M., Hylander, L. D., Daniel, G., & Heinmaa, I. (2020). Efficiency of iron-and calcium-impregnated biochar in adsorbing phosphate from wastewater in onsite wastewater treatment systems. *Front. Environ. Sci., 8*, 538539. https://doi.org/10.3389/fenvs.2020.538539

Feng, W., Gao, J., Cen, R., Yang, F., He, Z., Wu, J., Miao, Q., & Liao, H. (2020). Effects of polyacrylamide-based super absorbent polymer and corn straw biochar on the arid and semi-arid salinized soil. *Agriculture, 10*, 519. https://doi.org/10.3390/agriculture10110519

Grewal, J., & Khare, S. (2017). 2-Pyrrolidone synthesis from g-aminobutyric acid produced by Lactobacillus brevis under solid-state fermentation utilizing toxic deoiled cottonseed cake. *Bioprocess Biosyst. Eng., 40*, 145-152. https://doi.org/10.1007/s00449-016-1683-9

Grewal, J., Tiwari, R., & Khare, S. (2019). Secretome analysis and bioprospecting of lignocellulolytic fungal consortium for valorization of waste cottonseed cake by hydrolase production and simultaneous gossypol degradation. *Waste Biomass Valoriz., 11*, 2533-2548. https://doi.org/10.1007/s12649-019-00620-1

Guo, M., He, Z., & Uchimiya, S. M. (2016b). *Agricultural and Environmental Applications of Biochar: Advances and Barriers*. Soil Science Society of America, Inc., Madison, WI. https://doi.org/10.2136/sssaspecpub63

Guo, M., Labreveux, M., & Song, W. (2009). Nutrient release from bisulfate-amended phytase-diet poultry litter under simulated weathering conditions. *Waste Manage., 29*, 2151-2159. https://doi.org/10.1016/j.wasman.2009.02.012

Guo, M., Li, H., Baldwin, B., & Morrison, J. (2019). Thermochemical processing of animal manure for bioenergy and biochar. In Z. He, P. H. Pagliari & H. M. Waldrip (Eds.), *Animal Manure: Production, Characteristics, Environmental Concerns and Management* (pp. 255-274). American Society of Agronomy. Madison, WI. https://doi.org/10.2134/asaspecpub67.c21

Guo, M., Shen, Y., & He, Z. (2012). Poultry litter-based biochar: preparation, characterization, and utilization. In Z. He (Ed.), *Applied Research of Animal Manure: Challenges and Opportunities beyond the Adverse Environmental Concerns* (pp. 171-202). Nova Science Publishers, Inc. New York.

Guo, M., Uchimiya, S. M., & He, Z. (2016a). Agricultural and environmental applications of biochar: Advances and barriers. In Guo, M., He, Z., & Uchimiya, S. M. (Eds.), *Agricultural and Environmental Applications of Biochar: Advances and Barriers* (pp. 495-504). Soil Science Society of America, Inc., Madison, WI. https://doi.org/10.2136/sssaspecpub63.2014.0054

Haeldermans, T., Claesen, J., Maggen, J., Carleer, R., Yperman, J., Adriaensens, P., Samyn, P., Vandamme, D., Cuypers, A., & Vanreppelen, K. (2019). Microwave assisted and conventional pyrolysis of mdf-characterization of the produced biochars. *J. Anal. Appl. Pyrol., 138*, 218-230. https://doi.org/10.1016/j.jaap.2018.12.027

Han, Y. W. (1988). Removal of phytic acid from soybean and cottonseed meals. *J. Agric. Food Chem., 36*, 1181-1183. https://doi.org/10.1021/jf00084a014

He, Z., & Honeycutt, C. W. (2001). Enzymatic characterization of organic phosphorus in animal manure. *J. Environ. Qual., 30*, 1685-1692. https://doi.org/10.2134/jeq2001.3051685x

He, Z., & Mao, J. (2011). Functional groups identified by solid state ^{13}C NMR spectroscopy. In Z. He (Ed.), *Environmental Chemistry of Animal Manure* (pp. 41-59). Nova Science Publishers. NY.

He, Z., & Zhang, M. (2015). Structural and functional comparison of mobile and recalcitrant humic fractions from agricultural soils. In Z. He & F. Wu (Eds.), *Labile Organic Matter - Chemical Composition, Functions, and Significance in Soil and the Environment* (pp. 79-98). Soil Sci. Soc. Am. Madison, WI. https://doi.org/10.2136/sssaspecpub62.2014.0036

He, Z., Chapital, D. C., Cheng, H. N., & Dowd, M. K. (2014b). Comparison of adhesive properties of water- and phosphate buffer-washed cottonseed meals with cottonseed protein isolate on maple and poplar veneers. *Int. J. Adhes. Adhes., 50*, 102-106. https://doi.org/10.1016/j.ijadhadh.2014.01.019

He, Z., Chapital, D. C., Cheng, H. N., Klasson, K. T., Olanya, M. O., & Uknalis J. (2014a). Application of tung oil to improve adhesion strength and water resistance of cottonseed meal and protein adhesives on maple veneer. *Ind. Crop. Prod., 61*, 398-402. https://doi.org/10.1016/j.indcrop.2014.07.031

He, Z., Du, C., & Zhou, J. (2011). Structural and bonding environments derived from infrared spectroscopic studies. In Z. He (Ed.), *Environmental Chemistry of Animal Manure* (pp. 23-42). Nova Science Publishers. NY.

He, Z., Guo, M., Sleighter, R. L., Zhang, H., Fortier, C. A., & Hatcher, P. G. (2018). Characterization of defatted cottonseed meal-derived pyrolysis bio-oil by ultrahigh resolution electrospray ionization Fourier transform ion cyclotron resonance mass spectrometry. *J. Anal. Appl. Pyrol., 136*, 96-106. https://doi.org/10.1016/j.jaap.2018.10.018

He, Z., Honeycutt, C. W., Griffin, T. S., Cade-Menun, B. J., Pellechia, P. J., & Dou, Z. (2009a). Phosphorus forms in conventional and organic dairy manure identified by solution and solid state P-31 NMR spectroscopy. *J. Environ. Qual., 38*, 1909-1918. https://doi.org/10.2134/jeq2008.0445

He, Z., Honeycutt, C. W., Xing, B., McDowell, R. W., Pellechia, P. J., & Zhang, T. (2007). Solid-state Fourier transform infrared and ^{31}P nuclear magnetic resonance spectral features of phosphate compounds. *Soil Sci., 172*, 501-515. https://doi.org/10.1097/SS.0b013e318053dba0

He, Z., Klasson, K. T., Wang, D., Li, N., Zhang, H., Zhang, D., & Wedegaertner, T. C. (2016b). Pilot-scale production of washed cottonseed meal and co-products. *Mod. Appl. Sci., 10*(2), 25-33. https://doi.org/10.5539/mas.v10n2p25

He, Z., Mao, J., Honeycutt, C. W., Ohno, T., Hunt, J. F., & Cade-Menun, B. J. (2009b). Characterization of plant-derived water extractable organic matter by multiple spectroscopic techniques. *Biol. Fertil. Soils., 45*, 609-616. https://doi.org/10.1007/s00374-009-0369-8

He, Z., Ohno, T., Cade-Menun, B. J., Erich, M. S., & Honeycutt, C. W. (2006). Spectral and chemical characterization of phosphates associated with humic substances. *Soil Sci. Soc. Am. J., 70*, 1741-1751. https://doi.org/10.2136/sssaj2006.0030

He, Z., Olk, D. C., Tewolde, H., Zhang, H., & Shankle, M. (2020). Carbohydrate and amino acid profiles of cotton plant biomass products. *Agriculture, 10*, 2. https://doi.org/10.3390/agriculture10010002

He, Z., Pagliari, P. H., & Waldrip, H. M. (2016c). Applied and environmental chemistry of animal manure: A review. *Pedosphere, 26*, 779-816. https://doi.org/10.1016/S1002-0160(15)60087-X

He, Z., Uchimiya, S. M., & Guo, M. (2016a). Production and characterization of biochar from agricultural by-products: Overview and use of cotton biomass residues. In M. Guo, Z. He & S. M. Uchimiya (Eds.), *Agricultural and Environmental Applications of Biochar: Advances and Barriers* (pp. 63-86). Soil Science Society of America, Inc. Madison, WI. https://doi.org/10.2136/sssaspecpub63.2014.0037.5

He, Z., Zhang, H., & Olk, D. C. (2015b). Chemical composition of defatted cottonseed and soy meal products. *PLoS One, 10*(6), e0129933. https://doi.org/10.1371/journal.pone.0129933

He, Z., Zhang, H., Olk, D. C., Shankle, M., Way, T. R., & Tewolde, H. (2014c). Protein and fiber profiles of cottonseed from upland cotton with different fertilizations. *Mod. Appl. Sci., 8*(4), 97-105. https://doi.org/10.5539/mas.v8n4p97

He, Z., Zhang, H., Tewolde, H., & Shankle, M. (2017). Chemical characterization of cotton plant parts for multiple uses. *Agric. Environ. Lett., 2*, 110044. https://doi.org/10.2134/ael2016.11.0044

He, Z., Zhang, M., Cao, X., Li, Y., Mao, J., & Waldrip, H. M. (2015a). Potential traceable markers of organic matter in organic and conventional dairy manure using ultraviolet-visible and solid-state ^{13}C nuclear magnetic resonance spectroscopy. *Org. Agr., 5*, 113-122. https://doi.org/10.1007/s13165-014-0092-0

Jiang, Y., Ren, C., Guo, H., Guo, M., & Li, W. (2019). Speciation transformation of phosphorus in poultry litter during pyrolysis: Insights from X-ray diffraction, fourier transform infrared, and solid-state NMR spectroscopy. *Environ. Sci. Technol., 53*(23), 13841-13849. https://doi.org/10.1021/acs.est.9b03261

Johnson, R. L., & Schmidt-Rohr, K. (2014). Quantitative solid-State ^{13}C NMR spectra with signal enhancement by multiple cross-polarization. *J. Magn. Reson, 239*, 44-49. https://doi.org/10.1016/j.jmr.2013.11.009

Kalus, K., Koziel, J. A., & Opaliński, S. (2019). A review of biochar properties and their utilization in crop agriculture and livestock production. *Appl. Sci., 9*, 3494. https://doi.org/10.3390/app9173494

Li, F., Wu, X., Ji, W., Gui, X., Chen, Y., Zhao, J., Zhou, C., & Ren, T. (2020b). Effects of pyrolysis temperature on properties of swine manure biochar and its environmental risks of heavy metals. *J. Anal. Appl. Pyrol., 152*, 104945. https://doi.org/10.1016/j.jaap.2020.104945

Li, J., Pradyawong, S., He, Z., Sun, X. S., Wang, D., Cheng, H. N., & Zhong, J. (2019). Assessment and application of phosphorus/calcium-cottonseed protein adhesive for plywood production. *J. Clean. Prod., 229*, 454-462. https://doi.org/10.1016/j.jclepro.2019.05.038

Li, Q., Liu, X., Su, H., Mao, A., & Wan, H. (2020a) Improving performance of phenol-formaldehyde resins modified/blended with phenol-rich pyrolysis bio-oil. *Forest Prod. J., 70*, 387-395.

Liu, M., Wang, Y., Wu, Y., He, Z., & Wan, H. (2018). "Greener" adhesives composed of urea-formaldehyde resin and cottonseed meal for wood-based composites. *J. Clean. Prod., 187*, 361-371. https://doi.org/10.1016/j.jclepro.2018.03.239

Liu, Y., He, Z., & Uchimiya, M. (2015). Comparison of biochar formation from various agricultural by-products using FTIR spectroscopy. *Modern Appl. Sci., 9*(4), 246-253. https://doi.org/10.5539/mas.v9n4p246

Liu, Y., He, Z., Shankle, M., & Tewolde, H. (2016). Compositional features of cotton plant biomass fractions characterized by attenuated total reflection Fourier transform infrared spectroscopy. *Ind. Crop. Prod., 79*, 283-286. https://doi.org/10.1016/j.indcrop.2015.11.022

Liu, Y., Thibodeaux, D., & Gamble, G. (2011). Development of Fourier transform infrared spectroscopy in direct, non-destructive, and rapid determination of cotton fiber maturity. *Textile Res. J., 81*, 1559-1567. https://doi.org/10.1177/0040517511410107

Mahdi, Z., Hanandeh, A. E., & Yu, Q. (2017). Influence of pyrolysis conditions on surface characteristics and methylene blue adsorption of biochar derived from date seed biomass. *Waste Biomass Valor., 8*, 2061-2073. https://doi.org/10.1007/s12649-016-9714-y

Mao, A., He, Z., Wan, H., & Li, Q. (2017). Preparation, properties, and bonding utilization of pyrolysis bio-oil. In Z. He (Ed.), *Bio-based Wood Adhesives: Preparation, Characterization, and Testing* (pp. 260-279). CRC Press. Boca Raton, FL. https://doi.org/10.1201/9781315369242

Mao, J-D., Olk, D. C., Fang, X., He, Z., Bass, J., & Schmidt-Rohr, K. (2008). Influence of animal manure application on the chemical structures of soil organic matter as investigated by advanced solid-state NMR and FT-IR. *Geoderma, 146*, 353-362. https://doi.org/10.1016/j.geoderma.2008.06.003

Mao, J-D., & Schmidt-Rohr, K. (2004). Accurate quantification of aromaticity and nonprotonated aromatic carbon fraction in natural organic matter by ^{13}C solid state nuclear magnetic resonance. *Environ. Sci. Technol. 38*, 2680-2684. https://doi.org/10.1021/es034770x

Mok, W. S. L., Antal, M. J., Szabo, P., Varhegyi, G., & Zelei, B. (1992). Formation of charcoal from biomass in a sealed reactor. *Ind. Eng. Chem. Res., 31*, 1162-1166. https://doi.org/10.1021/ie00004a027

Nair, R. R., Mondal, M. M., & Weichgrebe, D. (2020). Biochar from co-pyrolysis of urban organic wastes—investigation of carbon sink potential using ATR-FTIR and TGA. *Biomass Conv. Bioref.* https://doi.org/10.1007/s13399-020-01000-9

Nam, S., Condon, B. D., Liu, Y., & He, Q. (2017). Natural resistance of raw cotton fiber to heat evidenced by the suppressed depolymerization of cellulose. *Polymer Degrad. Stabili, 138*, 133-141. https://doi.org/10.1016/j.polymdegradstab.2017.03.005

NFTS. (1993). Forage Analyses Procedures, National Forage Testing Association. Retrieved from https://fyi.extension.wisc.edu/forage/files/2014/01/NFTA-Forage-Analysis-Procedures.pdf

Noritomi, H., Kai, R., Endo, N., Kato, S., & Uchiyama, K. (2019). Thermal stabilization of HEWL by adsorption on biochar. *J. Mater. Sci. Res., 8*(4), 30-36. https://doi.org/10.5539/jmsr.v8n4p30

Noritomi, H., Nishigami, J., Endo, N., Kato, S., & Takagi, S. (2018). Effect of solvent on catalysis of protease adsorbed on biochar in organic media. *J. Mater. Sci. Res., 7*(4), 46-52. https://doi.org/10.5539/jmsr.v7n4p46

Noritomi, H., Nishigami, J., Endo, N., Kato, S., & Uchiyama, K. (2017). Influence of water activity on protease adsorbed on biochar in organic solvents. *J. Mater. Sci. Res., 6*(4), 96-102. https://doi.org/10.5539/jmsr.v6n4p96

Ozbay, N., Putun, A. E., & Putun, E. (2001). Structural analysis of bio-oils from pyrolysis and steam pyrolysis of cottonseed cake. *J. Anal. Appl. Pyrol., 60*(1), 89-101. https://doi.org/10.1016/S0165-2370(00)00161-3

Ozbay, N., Putun, A. E., & Putun, E. (2006). Bio-oil production from rapid pyrolysis of cottonseed cake: product yields and compositions. *Int. J. Energy Res., 30*(7), 501-510. https://doi.org/10.1002/er.1165

Perez-Mercado, L. F., Lalander, C., Berger, C., & Dalahmeh, S. S. (2018). Potential of biochar filters for onsite wastewater treatment: Effects of biochar type, physical properties and operating conditions. *Water, 10*, 1835. https://doi.org/10.3390/w10121835

Putun, E. (2010). Catalytic pyrolysis of biomass: effect of pyrolysis temperature, sweeping gas flow rate and MgO catalyst. *Energy, 35*, 2761-2766. https://doi.org/10.1016/j.energy.2010.02.024

Putun, E., Uzun, B. B., & Putnn, A. E. (2006). Production of bio-fuels from cottonseed cake by catalytic pyrolysis under steam atmosphere. *Biomass Bioenergy, 30*(6), 592-598. https://doi.org/10.1016/j.biombioe.2005.12.004

Ranatunga, T. D., He, Z., Bhat, K. N., & Zhong, J. (2017). Solid-state ^{13}C nuclear magnetic resonance spectroscopic characterization of soil organic matter fractions in a forest ecosystem subjected to prescribed burning and thinning. *Pedosphere, 27*, 901-911. https://doi.org/10.1016/S1002-0160(17)60439-9

Rodriguez, J. A., Lustosa Filho, J. F., Melo, L. C. A., de Assis, I. R., & de Oliveira, T. S. (2020). Influence of pyrolysis temperature and feedstock on the properties of biochars produced from agricultural and industrial wastes. *J. Anal. Appl. Pyrol., 149*, 104839. https://doi.org/10.1016/j.jaap.2020.104839

Schroder, J. L., Zhang, H., Richards, J. R., & He, Z. (2011). Sources and contents of heavy metals and other trace elements in animal manures. In Z. He (Ed.), *Environmental Chemistry of Animal Manure* (pp. 385-414). Nova Science Publishers. NY. https://doi.org/10.1002/agj2.20264

Singh, V., Soni, A., Kumar, S., & Singh, R. (2014). Characterization of liquid product obtained by pyrolysis of cottonseed de-oiled cake. *J. Biobased Mater. Bioenergy, 8*(3), 338-343. https://doi.org/10.1166/jbmb.2014.1445

Smidt, E., Lechner, P., Schwanninger, M., Haberhauer, G., & Gerzabek, M. H. (2002). Characterization of waste organic matter by FT-IR spectroscopy: application in waste science. *Appl. Spectrosc., 56*, 1170-1175. https://doi.org/10.1366/000370202760295412

Song, W., & Guo, M. (2012). Quality variations of poultry litter biochar generated at different pyrolysis temperatures. *J. Anal. Appl. Pyrol., 94*, 138-145. https://doi.org/10.1016/j.jaap.2011.11.018

Song, W., Kong, X., Hua, Y., Li, X., Zhang, C., & Chen, Y. (2020). Antioxidant and antibacterial activity and in vitro digestion stability of cottonseed protein hydrolysates. *LWT, 118*, 108724. https://doi.org/10.1016/j.lwt.2019.108724

Swiatkiewicz, S., Arczewska-Wlosek, A., & Jozefia, D. (2016). The use of cottonseed meal as a protein source for poultry: an updated review. *World Poultry Sci. J., 72*(3), 473-484. https://doi.org/10.1017/S0043933916000258

Waldrip, H. M., He, Z., Todd, R. W., Hunt, J. F., Rhoades, M. B., & Cole, N. A. (2014). Characterization of organic matter in beef feedyard manure by ultraviolet-visible and Fourier transform infrared spectroscopies. *J. Environ. Qual., 43*, 690-700. https://doi.org/10.2134/jeq2013.09.0358

Wan, H., Mao, A., Xu, W., Xi, E., & Li, Q. (2018). Evaluation of phenol formaldehyde resins modified/blended with pyrolysis bio-oil for plywood. *Forest Prod. J., 68*, 111-119. https://doi.org/10.13073/FPJ-D-17-00066

Windeatt, J. H., Ross, A. B., Williams, P. T., Forster, P. M., Nahil, M. A., & Singh, S. (2014). Characteristics of biochars from crop residues: Potential for carbon sequestration and soil amendment. *J. Environ. Manag., 146*, 189-197. https://doi.org/10.1016/j.jenvman.2014.08.003

Younis, U., Athar, M., Malik, S. A., Bokhari, T. Z., & Shah, M. (2017). Biochemical characterization of cotton stalks biochar suggests its role in soil as amendment and decontamination. *Adv. Environ. Res., 6*(2), 127-137. https://doi.org/10.12989/aer.2017.6.2.127

Zeng, X., Xiao, Z., Zhang, G., Wang, A., Li, Z., Liu, Y., Wang, H., Zeng, Q., Liang, Y., & Zou, D. (2018). Speciation and bioavailability of heavy metals in pyrolytic biochar of swine and goat manures. *J. Anal. Appl. Pyrol., 132*, 82-93. https://doi.org/10.1016/j.jaap.2018.03.012

Zhang, B., Cui, Y., Yin, G., Li, X. & You, Y. (2010). Synthesis and swelling properties of hydrolyzed cottonseed protein composite superabsorbent hydrogel. *Int. J. Polym. Mater. Polym. Biomater., 59*(12), 1018-1032. https://doi.org/10.1080/00914031003760709

Zhang, H., Vocase, F., Antonangelo, J., & Gillespie, C. (2020). Temporal changes of manure chemical compositions and environmental awareness in the Southern Great Plains. In Z. He, P. H. Pagliari & H. M. Waldrip (Eds.), *Animal Manure: Production, Characteristics, Environmental Concerns and Management* (pp. 15-26). American Society of Agronomy. Madison, WI. https://doi.org/10.2134/asaspecpub67.c2